Analytical Methods

Accepted Manuscript

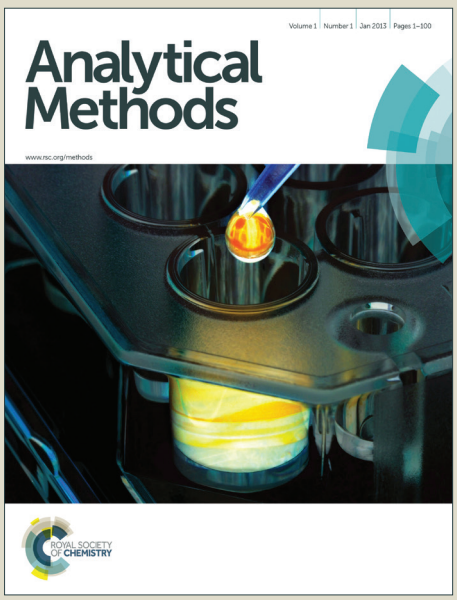

ROYAL SOCIETY OF CHEMISTRY

www.rsc.org/methods

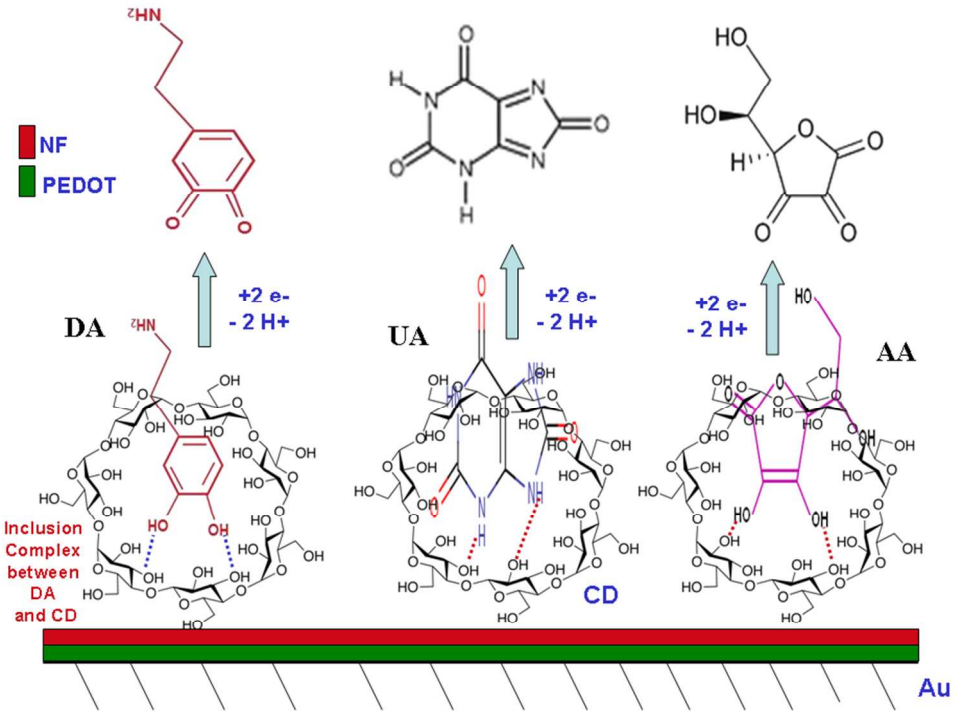

254x190mm (96 x 96 DPI)

Enhanced host-guest electrochemical sensing of dopamine in the presence of ascorbic and uric acids at β-cyclodextrin/Nafion®/Polymer nanocomposite

Nada F. Atta[*1], Ahmed Galal[1], Shimaa M. Ali[1], Dalia M. ElSaid[2]
[1]Department of Chemistry, Faculty of Science, Cairo University, 12613 Giza, Egypt
[2]Forensic Chemistry Laboratories, Medico Legal Department, Ministry of Justice, Cairo, Egypt

Tel: +20 02 35676561; fax: +20 02 35727556, nada_fah1@yahoo.com,

Abstract

A voltammetric method based on a combination of incorporated β-cyclodextrin (CD), Nafion® (NF) and poly(3,4-ethylene dioxy thiophene) (PEDOT) modified gold electrode Au/PEDOT/NF/CD has been successfully developed for determination of dopamine in presence of ascorbic acid (AA) and uric acid (UA). Optimization of the sensor was studied including the type of substrate, concentration of each modifier, pH of the electrolyte, method of deposition of the polymer and immobilization of CD and time of accumulation of the compound at the modified surface. Synergistic effect of high conductivity of PEDOT and Nafion® in addition to the pre-concentrating effect of β-cyclodextrin as well as its different host-guest inclusion complex and formation of hydrogen bonds with each compound was used to construct a stable electrochemical sensor for determination of these compounds. Under optimized conditions, linear calibration curve was obtained for determination of dopamine in urine in the range 0.6-320 μmol L^{-1} with correlation coefficient 0.996 and detection limit of 5.84 nmol L^{-1}. The proposed sensor was successfully used for simultaneous determinations of tertiary mixtures DA, AA and UA; DA, AA and acetaminophen (APAP) and binary mixture DA and ST. It has been demonstrated that Au/PEDOT/NF/CD can be used as sensor with excellent reproducibility, sensitivity and good stability.

***Keywords*:** Nafion®; Cyclodextrin; Sensor; Dopamine; Conducting Polymers; Host-Guest Complex.

1. Introduction:

Dopamine (DA) is an important neurotransmitter that is widely distributed in the mammalian central nervous system for massage transfer [1, 2]. DA plays a very important role in the functioning of central nervous, renal, hormonal and cardiovascular systems [3]. Neurological disorder such as Parkinson's disease and Schizophrenia may occur due to low levels of DA [1- 4]. Uric acid (UA) is another important biomolecule presents in urine and blood. It is the primary end product of purine metabolism. The very high levels of UA may indicate several diseases such as hyperuricemia, Lesch-Nyan disease and gout [5]. Ascorbic acid (AA), a vital vitamin in human diet and very popular for its antioxidant properties, exists in both animal and plant kingdoms. Many diseases are prevented and treated using AA such as common cold, mental illness, infertility and cancer and even in some clinical manifestation of human immunodeficiency virus (HIV) infections [5]. The simultaneous detection of DA, AA and UA has high importance in both the biomedical chemistry and neurochemistry and in the field of diagnostic and pathological research. The simultaneous determination of DA, AA and UA at conventional solid electrodes (carbon and metal) usually undergoes an overlapping oxidation potential and electrode fouling due to the adsorption of oxidation products [6]. The determination of these compounds using simple and rapid detection is a must without cross-interference, so that electrochemical methods were considered. They are less time consuming, more selective, less expensive and can be applied to a real-time determination in vivo [7]. Different approaches have been utilized for the electrochemical detection of dopamine such as self-assembled monolayers of omegamer-capto carboxylic acid [8], Au-carbon dots-chitosan modified glassy carbon electrode [9] and carbon nanotube modified microelectrode [10].

Conducting polymers are widely used as coating in fabrication of electro-sensors. Among polythiophenes, poly(3,4-ethylenedioxythiophene) (PEDOT) is the most studied one [11, 12]. PEDOT has proved to adhere strongly on most electrode materials, present good stability in aqueous electrolytes, show high conductivity in its oxidized state, have biocompatibility with biological media, and resist fouling by the oxidation products, thus PEDOT is very promising in the design of an electrochemical sensor [13- 18].

Nafion® (NF), a per-fluorinated sulfonated cation exchanger, consists of a linear backbone of fluorocarbon chains and ethyl ether pendant groups with sulfonic cation exchange sites which are highly permeable to cations but almost impermeable to anions. It presents many advantages such as high chemical and thermal stability, chemical inertness and mechanical strength. NF is widely used to modify electrodes in electrochemistry particularly in biosensors, due to its easy fabrication, good electrical conductivity, good adhesion on the electrode surface, improvement of the anti-interferential ability of the sensor and high partition coefficients of many redox compounds in NF [19-28]. The accumulation mechanism of NF can be explained through an electrostatic interaction due to the hydrophilic negatively charged sulfonate groups in the polymer structure, whereas its ionic selectivity for hydrophobic organic cations is achieved through hydrophobic interactions with the hydrophobic fluorocarbons of the film [29, 30]. NF films allow the electrolytes to proceed while preventing adsorption-desorption processes of organic species. NF preconcentrates positively charged molecules, which increases the sensitivity of the measurements while retaining ionic selectivity for hydrophobic organic cations [29-34].

There is another attractive electrode modifier belongs to the cyclodextrin family due to their structural characteristics and special functions [35-39]. They are cyclic oligosaccharides consisting of six, seven or eight glucose units called α-, β- and γ-cyclodextrins [40-42]. These CDs possesses a hydrophobic inner cavity and a hydrophilic outer tail and form stable host-guest inclusion complexes or nanostructure supramolecular assemblies with suitable organic, inorganic, neutral and ionic substances resulting in the design of selective electrodes [43-49]. β-cyclodextrin (CD) is composed of α-1,4 linked glucopyranose subunit [43, 50-55] and has many advantages such as good biocompatibility and adsorption capabilities directly on solid surfaces. It has been applied in many fields such as electrochemical sensor, catalysis, enzyme mimics, biological systems, molecular recognition and increasing solubility and dispersibility [50, 53, 54].

In this work, the electrochemical oxidation behavior of DA was investigated for the first time at Au/PEDOT/NF/CD composite electrode. Based on the excellent properties of PEDOT, CD and NF, the utilized sensor facilitated the electron transfer of

DA resulting in enhancement of the oxidation signals. The performance of the fabricated electrode such as sensitivity, linear range and selectivity is evaluated and discussed. Moreover, the proposed sensor was investigated for the simultaneous determination of DA, AA and UA. The applicability of the electrode is demonstrated for determination of DA in real samples.

2. Experimental

2.1. Materials and reagents

All chemicals were used as received without further purification. 3,4-ethylene dioxy-thiophene (EDOT), tetrabutylammonium hexafluorophosphate (Bu_4NPF_6), acetonitrile, ([HPLC] grade), lithium perchlorate ($LiClO_4$), dopamine (DA), uric acid (UA), ascorbic acid (AA), Nafion® (NF) and β-cyclodextrin (CD) were supplied by Aldrich Chem. Co. (Milwaukee, WI, USA). Phosphate buffer solution 0.1 mol L^{-1} PBS (1 mol L^{-1} K_2HPO_4 and1 mol L^{-1} KH_2PO_4) was used as the supporting electrolyte. pH was adjusted using 0.1 mol L^{-1} H_3PO_4 and 0.1 mol L^{-1} KOH. All solutions were prepared using double distilled water.

2.2. Electrochemical cells and equipments:

Electrochemical polymerization and characterization were carried out with a three electrode/one-compartment glass cell. It was connected to the electrochemical workstation from BAS-100B electrochemical analyzer (Bioanalytical Systems, BAS, West Lafayette, USA). The working electrode was gold disc (diameter: 1.5 mm). A 6.0 cm platinum wire from BAS was employed as auxiliary electrode. All the cell potentials were measured with respect to Ag/AgCl (4 mol L^{-1} KCl saturated with AgCl) reference electrode from BAS. Working electrode was polished using alumina (2 μM)/water slurry until no visible scratches were observed. Prior to immersion in the cell, the electrode surface was thoroughly rinsed with distilled water and dried. All experiments were performed at 25± 0.2 °C. The electrochemical impedance spectroscopy was performed using a Gamry-750 system and a lock-in-amplifier that are connected to personal computer. The data analysis software was provided with the instrument and applied non linear least square fitting with Levenberg-Marquardt algorithm. All impedance

experiments were recorded between 0.1 Hz and 100 kHz. Quanta FEG 250 instrument was used to obtain the scanning electron micrographs.

2.3. Construction of the proposed sensor

Bulk Electrolysis (BE) was employed for deposition of the polymer film from a solution of 0.001 M EDOT and 0.05 M Bu_4NPF_6 in acetonitrile. The potential applied between gold disc working electrode and the reference (Ag/AgCl) was held constant at +1.4 V for 10 s (the optimized time). The electrode was represented as Au/PEDOT. Then 10 µL (the optimized volume) of 2% Nafion® (NF) (the optimized concentration) was added on Au/PEDOT electrode. The electrode was left for 15 to 20 min in open air to allow the NF film to dry. The utilized electrode is represented as Au/PEDOT/NF. Finally, an outer film of cyclodextrin (CD) was formed electrochemically via Bulk electrolysis (the optimized method). The potential applied between the working electrode and the reference (Ag/AgCl) was held constant at +1.2 V for 3 min (the optimized time) in a solution of 10^{-5} M CD (the optimized concentration) in 0.05 M $LiClO_4$. The proposed sensor is represented as Au/PEDOT/NF/CD.

2.4. Analysis of urine

The utilization of the proposed method in real sample analysis was also investigated by direct analysis of DA in human urine samples. DA was dissolved in urine to make a stock solution with 1 mmol L^{-1} concentration. Standard additions were carried out from the DA stock solution in 15 mL of 0.1 mol L^{-1} PBS (pH 7.40).

3. Result and discussion

3.1. Optimization of preparation conditions

Two electrochemical methods were employed for deposition of the polymer film on the Au electrode; bulk electrolysis (BE) and cyclic voltammetery (CV). For BE, the potential applied between gold disc working electrode and the reference (Ag/AgCl) was held constant at +1.4 V for 5, 10 and 15 sec. In case of CV, the potential was cycled between -0.2 and +0.7 V at a scan rate 50 mV s^{-1} and the amount of electrodeposited polymer film was controlled by the number of cycles; 3, 5 and 10 cycles. The resulting films were tested in 1 mM DA/0.1 M PBS/pH 7.40. Au/PEDOT(BE) gives higher catalytic activity

toward DA oxidation than Au/PEDOT(CV). Moreover, the effect of deposition time was investigated and the film formed via BE for 10 s gives the highest electrocatalytic activity toward DA than other conditions. On the other hand, the effect of concentration of NF solution that used to form NF film on PEDOT was studied and the test was achieved using Au/PEDOT/NF (with different concentration)/CD in 1 mM DA/0.1 M PBS/pH 7.40. The 2% NF gives the best catalytic activity toward DA oxidation. Moreover, CD immobilization was achieved using three methods; soaking of electrode in CD solution with different concentrations, chemical addition of different volumes on the top of the electrode and bulk electrolysis for different time (Fig. 1A). The test was achieved using Pt/PEDOT/CD (chemically, soaking, electrochemically) in 1 mM DA/0.1 M PBS/pH 7.40. The film formed via bulk electrolysis for 3 min in 10^{-3} M of CD solution gives the best response toward DA oxidation.

On the other hand, the effect of substrate was studied. The composite was formed on gold (Au) and platinum (Pt) substrates (Fig. 1B). The test was achieved using Au/PEDOT/NF/CD and Pt/PEDOT/NF/CD in 1 mM DA/0.1 M PBS/pH 7.40. Higher response toward DA oxidation was achieved in case of Au due to the higher catalytic activity of Au substrate.

Insert Fig. 1 (A, B)

3.2. Electrochemistry of DA at Au/PEDOT/NF/CD

Fig. 2 compares typical cyclic voltammograms of 1 mM DA/ 0.1 M PBS/ pH 7.40 recorded at four different working electrodes (bare Au, Au/PEDOT(BE), Au/PEDOT(BE)/NF, Au/PEDOT(BE)/CD(BE) and Au/PEDOT(BE)/NF/CD(BE)). A poorly defined oxidation peak was observed at 442 mV at bare Au electrode, whereas the potential shifts negatively to 350 and 209 mV at Au/PEDOT/NF and Au/PEDOT electrodes, respectively. Moreover, the oxidation peak current increases from 4.33 µA at bare Au to 5.37 µA and 16.6 µA at Au/PEDOT/NF and Au/PEDOT electrodes, respectively. The anodic peak shifted to 210 mV at Au/PEDOT/CD and the oxidation peak current increases to 27.5 µA. On the other hand, high oxidation peak current 42.75 µA was observed at Au/PEDOT/NF/CD at 220 mV (Table 1). When compared to bare

Au electrode, the oxidation current of DA increases by 1.2, 4, 6 and 10 folds at Au/PEDOT/NF, Au/PEDOT, Au/PEDOT/CD and Au/PEDOT/NF/CD, respectively which indicates the catalytic DA oxidation at the proposed composite. An increase in the oxidation peak current and enhancement of the direct electron transfer of DA was observed at Au/PEDOT/NF/CD due to the synergistic effect of polymer, NF and CD films. The previous results could be interpreted as following; PEDOT film has a rich electron cloud acting as an electron mediator. Moreover, a distribution of hydrophobic (reduced) and hydrophilic (oxidized) regions exists in the PEDOT film and the hydrophobic DA^+ cations prefer to interact with the more hydrophobic regions favoring reversible oxidation of DA [15]. On the other hand, the NF film can enhance the surface preconcentration of DA via ion-exchange, accumulations of DA in the hydrophilic regions or the ion channels of NF. This results in improvement of selectivity and sensitivity at the Nafion® film coated electrode [29-31, 33]. Furthermore Nafion® increases the electrical conductivity of the composite beside it works as suitable layer for forming the CD in it due to its good adhesion at the polymer surface. So upon the modification of Au/PEDOT/NF with CD film, a supramolecular host-guest inclusion complex is formed between β-CD and DA via electrostatic, inclusion interactions and hydrogen bonds formation, thus a selectivity advantage is achieved through the formation of such complex, resulting in enhancement of the charge transfer properties of DA [47-51, 53-55]. The presence of β-CD results in significant increase in oxidation signal of DA which is an indicative of the penetration of DA into the relatively less polar cavity of β-CD and formation of DA:CD inclusion complex [44, 47]. Scheme 1 illustrates the inclusion complex and formation of hydrogen bonds between DA and β-CD which enhances the electrochemical oxidation of DA into DA-o-quinone and facilitates the electron transfer process.

Insert Fig. 2, Scheme 1 and Table 1

3.3. Surface morphology

The physical morphology of the surface affected the response of an electrochemical sensor. An obvious difference was observed between Au/PEDOT and Au/PEDOT/NF/CD as shown in Fig. 3 (A, B); respectively. PEDOT film (Fig. 3 A) has

globular morphology and the surface looks rough due to the Au substrate. On the other hand, Au/PEDOT/NF/CD exhibits unique morphology with highly porous surface resulting in greater specific surface area, faster electron transfer, enhancement of the contact area with the analytes and thus, higher catalytic activity.

Insert Fig. 3 (A, B)

3.4. Effect of accumulation time

The sensitivity of the proposed method was improved by the accumulation time. The effect of accumulation time on the oxidation peak currents of DA at Au/PEDOT/NF/CD was investigated from 0 to 120 s (Fig. 4). The oxidation peak currents increased sharply within the first 20 s, decreased at 40 s. With further increasing accumulation time, the oxidation peak current increased slightly but with values smaller than that at 20 s then reaching a limiting value. The optimum accumulation time is 20 s [44].

Insert Fig. 4

3.5. Effect of scan rate

The dependence of the anodic peak current (I_{pa} A) on the scan rate has been used for the estimation of the "apparent" diffusion coefficient D_{app} of 1 mM DA/0.1 M PBS/pH 7.40. D_{app} ($cm^2\ s^{-1}$) values were calculated from Randles Sevcik equation:

$$I_{pa} = (2.69 \times 10^5)\ n^{3/2} A C_o D^{1/2} \nu^{1/2}$$

where n is the number of electrons exchanged in oxidation at T = 298 K, A is the geometrical electrode area = 0.0177 cm^2, C_o is the analyte concentration (1×10^{-6} mol cm^{-3}) and ν is the scan rate V s^{-1}. It is important to notice that the apparent surface area used in the calculations does not take into account the surface roughness, which is inherent characteristic for all polymer films formed using the electrochemical techniques. Supplement 1 shows the CVs of 1 mmol L^{-1} DA/0.1 mol L^{-1} PBS/pH 7.40 at Au/PEDOT/NF/CD at different scan rates (from 10 mV s^{-1} up to 200 mV s^{-1}). It can be noticed that a pair of roughly symmetric anodic and cathodic peaks appeared with almost equal peak currents. Moreover, the anodic and cathodic peak currents and the peak-to-peak separation increased with increasing the scan rate. For a diffusion-controlled

process, a plot of the anodic peak current values versus the square root of the scan rate results in a straight-line relationship and the inset of Supplement 1 shows this linear relationship for DA at Au/PEDOT/NF/CD. D_{app} values are 2.07×10^{-6}, 3.18×10^{-6}, 3.04×10^{-5}, 8.34×10^{-5} and 2.02×10^{-4} at bare Au, Au/PEDOT/NF, Au/PEDOT, Au/PEDOT/CD and Au/PEDOT/NF/CD, respectively (Table 1). These values indicate the catalytic DA oxidation at the proposed composite.

3.6. Effect of solution pH

The effect of changing the pH of the supporting electrolyte on the electrochemical response of DA was studied (Fig. not shown). It is clear that changing the pH of the supporting electrolyte altered both the peak potentials and the peak currents of DA. Both the anodic and the cathodic peak potentials shifted negatively with the increase in the solution pH, indicating that the electrocatalytic oxidation of DA at Au/PEDOT/NF/CD is a pH-dependent reaction and protonation/deprotonation is taking part in the charge transfer process. Supplement 2 shows the relationship between the anodic peak potential and the solution pH value (over the pH range of 2–11) could be fit to the linear regression equation with a correlation coefficient of $R^2 = 0.972$.

$$E_{pa}\,(V) = (0.621) - (0.052)\,pH$$

The slope was −0.052 V/pH units over the pH range 2–11, which is close to the theoretical value of −0.059 V/pH. This indicated that the number of protons and transferred electrons involved in the oxidation mechanism is equal. As the DA oxidation is a two-electron process, the number of protons involved was also predicted to be two indicating a 2e−/2H+ process. In solution, the pKa values of DA are 8.90 (pK_{a1}) and 10.6 (pK_{a2}). Inset of Supplement 2 shows the relationship between the anodic peak current and the solution pH value, the anodic peak current increased from pH 2 to pH 7.40 where it reached its maximum value and decreased again at pH 9.00. The highest oxidation peak current was obtained at pH 7.40 (pH medium of the human body).

3.7. Determination of DA at physiological pH using Au/PEDOT/NF/CD

The voltammetric behavior of DA was examined using differential pulse voltammetry (DPV). Fig. 5 shows typical DPV of standard additions of 0.5 mmol L^{-1} DA/0.1 mol L^{-1} PBS/pH 7.40 in 15 mL of 0.1 mol L^{-1} PBS/pH 7.40 at Au/PEDOT/NF/CD. Fig. 5 shows that by increasing the concentration of DA, the anodic peak current increases which indicates that the electrochemical response of DA is apparently improved at Au/PEDOT/NF/CD due to the enhanced accumulation of protonated DA. The inset of Fig. 5 shows the calibration curve of the anodic peak current values in the linear range of 2–320 μmol L^{-1} DA with the regression equation:

$$Ip\ (A) = (5.205 \times 10^{-6}) + 0.1191 \times 10^{-6}\ c\ (\mu mol\ L^{-1})$$

and with correlation coefficient of 0.9955, sensitivity of 0.1191 μA/ μmol L^{-1} and detection limit of 2.52 nmol L^{-1}. The detection limit (DL) was calculated from:

$$DL = 3s/b$$

Where s is the standard deviation and b is the slope of the calibration curve. Table 2 shows the comparison for the determination of DA at Au/PEDOT/NF/CD with various modified electrodes based in literature reports. The proposed sensor showed the excellent features, such as wide linear response range, high sensitivity and selectivity, good reproducibility and long time stability.

Insert Fig. 5 and Table 2

3.8. Determination of DA in human urine samples

The utilization of the proposed method in real sample analysis was also investigated by direct analysis of DA in human urine. The same measurements were conducted successfully on urine samples. In this set of experiments, DA was dissolved in urine to make a stock solution with 0.5 mmol L^{-1} concentration. The detection limit of 5.84 nmol L^{-1} with correlation coefficient of 0.996 is obtained in the linear range of 0.6-320 μmol L^{-1}. Four different concentrations on the calibration curve are chosen to be repeated to evaluate the accuracy and precision of the proposed method, which is represented in Table 3. The recovery ranged from 98.8 % to 100.3 %, and the results are acceptable indicating that the present procedures are free from interferences of the urine sample

matrix. The results strongly proved that DA can be selectively and sensitively determined at Au/PEDOT/NF/CD modified electrode in urine sample. This sensor proved to be successfully used for DA determination in pharmaceutical and clinical preparations.

Insert Table 3

3.9. Effect of interferences on the determination of DA

It is well known that DA, AA and UA coexist in the extracellular fluid of the central nervous system and serum. Au/PEDOT/NF/CD sensor was evaluated for the simultaneous voltammetric determination of DA, AA and UA in their mixture. Fig. 6 A and the inset show the DPVs of 300 μmol L^{-1} DA, 5 mmol L^{-1} AA and 500 μmol L^{-1} UA in 0.1 M PBS/pH 7.40 at Au/PEDOT/NF/CD and bare Au, respectively. An overlapped voltammetric peak was obtained at bare Au at 328 mV. However, simultaneous determination of DA, AA and UA is achieved at the proposed sensor due to the catalytic activity of PEDOT, Nafion® and cyclodextrin films. Three well resolved oxidation peaks appear at Au/PEDOT/NF/CD at -24, 192 and 328 mV for AA, DA and UA, respectively. The large peak separation of the anodic peaks of DA, AA and UA is enough to allow simultaneous determination of mixture solutions. It was found that owing to the synergetic effect of PEDOT, NF and CD at Au/PEDOT/NF/CD, the electro-oxidation of each molecule became facile and distinguishable at the surface of Au/PEDOT/NF/CD. On the other hand, Acetaminophen (paracetamol), APAP, is also likely to interfere with DA and AA determination. Simultaneous voltammetric determination of DA, AA and APAP in their mixture was achieved at Au/PEDOT/NF/CD. Fig. 6 B shows the DPV of 500 μmol L^{-1} DA, 1 mmol L^{-1} AA and 500 μmol L^{-1} APAP in 0.1 M PBS/pH 7.40 at Au/PEDOT/NF/CD. Three resolved peaks were obtained at -20, 170 and 370 mV for AA, DA and APAP, respectively. On the other hand, DA is a typical neurotransmitter which coexists with ST at the close level in the brain [26] thus, the simultaneous determination of ST and DA should be investigated. The inset of Fig. 6 B shows the voltammetric separation of 1 mM DA and 1 mM ST in 0.1 M PBS/pH 7.40 at Au/PEDOT/NF/CD. Two voltammetric peaks appeared at 160 and 340 mV for DA and ST, respectively. One can say that DA and ST don't interfere with each other at the proposed sensor [44]. All cases of mixtures showed good separation of their components with a good potential peak

separation between them. Another conclusion can be withdrawn from the above results is the simultaneous determination of all mixtures was achieved via the inclusion of the compounds of every mixture in the CD cavities and formation of a stable host-guest complexes which enhances the electron transfer process (scheme 1).

Insert Fig. 6 (A, B)

3.10. Stability of the proposed sensor

The stability of Au/PEDOT/NF/CD was studied via repeated cycles up to 50 cycles. Supplement 3 shows the repeated cycles up to 50 cycles of Au/PEDOT/NF/CD in 1 mmol L^{-1} DA/0.1 mol L^{-1} PBS/pH 7.40. Excellent stability without any noticeable decrease in the current response was obtained. Thus, both anodic and cathodic peak currents remained relatively stable indicating that this modified electrode has a good reproducibility and does not suffer from surface fouling during the repetitive voltammetric measurement.

3.11. Electrochemical impedance spectroscopy

The interface properties of the modified surface were effectively studied using electrochemical impedance spectroscopy (EIS). EIS data were obtained at ac frequency varying between 0.1 Hz and 100 kHz. The EIS measurements were carried out in a background solution of 1 mM DA in 0.1 M PBS/ pH 7.40 at 440 mV and 215 mV; the oxidation potentials of DA at bare and modified electrode, respectively. Fig. 7 and the inset show the typical impedance spectra presented in the form of Nyquist plot for modified and bare electrode, respectively. The experimental data were compared to an equivalent circuit that used some of the conventional circuit elements (inset of Fig. 7). In this circuit, Rs is the solution resistance and Rct is the charge transfer resistance. CPE1 and CPE2 represent the predominant diffusion influence on the charge transfer process and n and m are their corresponding exponents (n and m less than one). Cf and Cc represent the capacitance of the double layer and W is the Warburg impedance due to diffusion. Table 4 lists the best fitting values calculated from the equivalent circuit for the impedance data.

The impedance spectra include a semicircle portion at the higher frequencies corresponding to the electron-transfer-limiting electrochemical process and a linear portion at the lower frequencies corresponding to diffusion-limiting electrochemical process. The semicircle diameter represents the interfacial charge transfer resistance Rct which controls the electron transfer kinetics of the redox probe at the electrode interface. Thus, Rct describes the interface properties of the electrode. In more details, the impedance spectra include a semicircle part with larger diameter with Rct equals 4210 Ω cm^2 in case of bare Au. The diameter of semicircle for the modified electrode diminishes markedly and Rct decreases greatly (132.3 Ω cm^2) thus, the charge transfer rate is enhanced. The presence of PEDOT, NF and CD played an important role in the obvious decrease of Rct and facilitation of charge transfer. As well, value of Warburg impedance due to diffusion (W) for bare Au is 5.302×10^4 Ω $s^{-1/2}$ which decreases greatly to 1.566×10^2 Ω $s^{-1/2}$ for modified electrode, indicating less electronic resistance and more facilitation of charge transfer.

Insert Fig. 7 and Table 4

4. Conclusions

Employing conducting polymer PEDOT, NF, CD as modifiers for Au electrode, an electrochemical sensor has been developed for determination of DA concentration using the voltammetry technique**.** Synergistic effect of high conductivity of PEDOT and Nafion® in addition to the preconcentrating effect of β-cyclodextrin as well as its different host guest inclusion complexes and formation of hydrogen bonds with each compound was used to construct a stable electrochemical sensor. This optimized sensor is used for simultaneous determination of tertiary mixture DA, AA and UA; DA, AA and APAP and binary mixture of DA and ST. The method described is rapid, simple, sensitive and successfully applied for direct determination of DA in human urine samples with excellent recovery results. Furthermore, the sensor showed good stability, high reproducibility, anti-interference ability and low detection limit.

5. Acknowledgment

The authors would like to acknowledge the financial support from Cairo University through the Vice President Office for Research Funds.

6. References

[1] N. F. Atta, A. Galal, F. M. Abu-Attia, S. M. Azab, *J. Electrochem. Soc.*, 2010, **157 (9)**, F116- F123.

[2] S. Thiagarajan, S. Chen, *Talanta*, 2007, **74**, 212-222.

[3] P. Damier, E. C. Hirsch, Y. Agid, A. M. Graybiel, *Brain,* 1999, **122**, 1437-1448.

[4] R. M. Wightman, L. J. May, A. C. Micheal, *Anal.Chem.,* 1988, **60 (13)**, 769A-779A.

[5] O. Arrigoni, M. C. Tullio, *Biochim. Biophys. Acta.,* 2002, **1569**, 1-9.

[6] H. R. Zare, N. Nasirizadeh, M. M. Ardakani, *J. Electranal. Chim.*, 2005, **577**, 25-33.

[7] Z. Gao, K.S. siow, A. Ng, Y. zhang, *Anal. Chim. Acta*., 1997, **343**, 49-57.

[8] F. Malem, D. Mandler, Analytical Chemistry, 1993, **65 (1)**, 37-41.

[9] Q. Huang, H. Zhang, S. Hu, F. Li, W. Weng, J. Chen, Q. Wang, Y. He, W. Zhang, X. Bao, *Biosens. Bioelectron.*, 2014, **52**, 277-280.

[10] B. E. K. Swamy, B. J. Venton, *Analyst*, 2007, **132**, 876-884.

[11] B. Rajesh, K. R. Thampi, J. M. Bornard, A. J. McEvoy, N. Xanthopoulos, H. J. Mathieu, B. Viswanathan, *J. Power Sources.,* 2004, **133**, 155-161.

[12] X. Huang, Y. Li, Y. Chen, L. Wang, *Sens. Actuators B*., 2008, **134**, 780-786.

[13] C. Y. Lin, V. S. Vasantha, K. C. Ho, *Sens. Actuators, B.,* 2009, **140**, 51–57.

[14] F. S. Belaidi, D. Evrard, P. Gros, *Electrochem. Commun.,* 2011, **13**, 423–425.

[15] N. F. Atta, A. Galal, R. A. Ahmed, *Bioelectrochemistry*, 2011, **80**, 132–141.

[16] A. Kros, N. A. J. M. Sommerdijk, R. J. M. Nolte, *Sens. Actuators, B.,* 2005, **106**, 289–295.

[17] A. R. Gonçalves, M. E. Ghica, C. M. A. Brett, *Electrochim. Acta*., 2011, **56**, 3685–3692.

[18] F. S. Belaidi, P. T. Boyer, P. Gros, J. *Electroanal. Chem.,* 2010, **647**, 159–168.

[19] H. C. Yi, K. B. Wu, S. S. Hu, D. F. Cui, *Talanta,* 2001, **55**, 1205–1210.

[20] P. Luo, G. Xie, Y. Liu, H. Xu, S. Deng, F. Song, *Clin. Chem. Lab. Med.,* 2008, **46**, 1641–1647.

[21] P.Y. Chen, R. Vittal, P. C. Nien, K. C. Ho, *Biosens. Bioelectron.,* 2009, **24**, 3504–3509.

[22] G. Nagy, G. A. Gerhardt, A. F. Oke, M. E. Rice, R. N. Adams, M. N. Szentirmay, C. R. Martin, *J. Electroanal. Chem.,* 1985, **188**, 85–94.

[23] Y. Chen, T. C. Tan, *Talanta*, 1995, **42**, 1181–1188.

[24] M. M. Dávila, M. P. Elizalde, J. Mattusch, R. Wennrich, *Electrochim. Acta*., 2001, **46**, 3189–3197.

[25] S. Yuan, S. Hu, *Electrochim. Acta*., 2004, **49**, 4287–4293.

[26] C. Gouveia-Caridade, C. M. A. Brett, *Electroanalysis*, 2005, **17**, 549-555.

[27] S. Tan, D. Bélanger, *J. Phys. Chem. B.,* 2005, **109**, 23480-23490.

[28] T. Lu, I. Sun, *Electroanalysis,* 2000, **12**, 605-609.

[29] N. F. Atta, A. Galal, S. M. Azab, *J. Electrochem. Soc.,* 2012, **159 (10)**, H765-H771.

[30] N. F. Atta, A. Galal, S. M. Azab, *Analyst*, 2011, **136**, 4682- 4691.

[31] N. F. Atta, A. Galal, F. M. Abu-Attia, S. M. Azab, *J. Mater. Chem.*, 2011, **21**, 13015-13024.

[32] D. P. Quana, D. P. Tuyena, T. D. Lamb, P. T. N. Trama, N. H. Binh, P. H. Viet, *Colloids Surf., B.,* 2011, **88**, 764–770.

[33] A. Babaei, A. R. Taheri, *Sens. Actuators, B.,* 2013, **176**, 543–551.

[34] S. Ku, S. Palanisamy, S. Chen, *J. Colloid Interface Sci.*, 2013, **411**, 182-186.

[35] X. Tiana, C. Cheng, H. Yuan, J. Dua, D. Xiao, S. Xie, M. M. F. Choi, *Talanta*, 2012, **93**, 79–85.

[36] Y. Wu, Z. Dou, Y. Liu, G. Lv, T. Pu, X. He, *RSC Adv.,* 2013, **3**, 12726-12734.

[37] D. Jia, J. Daib, H. Yuana, L. Lei, D. Xiao, *Talanta*, 2011, **85**, 2344–2351.

[38] M. L. Bender and M. Komiyama, Cyclodextrin Chemistry, Springer-Verlag, Berlin, Heidelberg, New York, 1978, pp. 701–702.

[39] W. Saenger, (Eds: J. S. Zejtli), Proceedings of the First International Symposim on Cyclodextrin, D. Reidel Rublishing Company Press, Hungary, 1982, pp. 141.

[40] P. He, J. Ye, Y. Fang, I. Suzuki, T. Os, *Anal. Chim. Acta.,* 1997, **337**, 217-223.

[41] A. Ferancová, E. Korgová, T. Buzinkaiová, W. Kutner, I. Štěpánek, J. Labud, *Anal. Chim. Acta*., 2001, **447**, 47–54.

[42] Y. Hu, Z. Zhang, H. Zhang, L. Luo, S. Yao, *Talanta*, 2011, **84**, 305–313.

[43] A. Ueno, I. Suzaki, T. Osa, *Anal. Chem.*, 1990, **62**, 2461-2466.

[44] A. Abbaspour, A. Noori, *Biosens. Bioelectron.*, 2011, **26**, 4674–4680.

[45] A. J. Bard and L. R. Falkner, Electrochemical Methods; Fundamentals and Applications, Wiley, New York, 2001.

[46] C. C. Harley, A. D. Rooney, C. B. Breslin, *Sens. Actuators*, B., 2010, **150**, 498–504.

[47] G.A. Angeles, B. Pérez-López, M. E. Palomar-Pardave, M. T. Ramírez-Silva, S. Alegret, A. Merkoçi, *Carbon*, 2008, **46**, 898-906.

[48] M. T. Ramirez-Silva, S. Corona-Avendaño, G. Alarcón-Angelesc, A. Rojas-Hernández, M. A. Romero-Romo and M. Palomar-Pardavé, *ECS Trans.*, 2009, **20 (1)**,151-157.

[49] M. Palomar-Pardavé, G. Alarcón-Angelesc, S. Corona-Avendaño, M. A. Romero-Romo, A. Merkoçi, A. Rojas-Hernández, M. T. Ramirez-Silva, *ECS Trans.,* 2011, **36(1)**, 471-481.

[50] W. Lian, J. Huang, J. Yu, X. Zhang, Q. Lin, X. He, X. Xing, S. Liu, *Food Control,* 2012, **26**, 620-627.

[51] D. Bouchta, N. Izaoumen, H. Zejli, M. El Kaoutit, K. R. Temsamani, *Biosens. Bioelectron.*, 2005, **20**, 2228–2235.

[52] X. Xu, Z. Liu, X. Zhang, S. Duan, S. Xu, C. Zhou, *Electrochim. Acta*., 2011, **58**, 142–149.

[53] H. Wanga, Y. Zhou, Y. Guo, W. Liu, C. Dong, Y. Wu, S. Li, S. Shuang, *Sens. Actuators*, B., 2012, **163**, 171–178.

[54] A. Cao H. Ai, Y. Ding, C. Dai, J Fei, *Sens. Actuators*, B., 2011, **155**, 632–638.

[55] J. Han, K. Huang, J. Li, Y. Liu, M. Yu, *Colloids Surf., B.,* 2012, **98**, 58–62.

List of Figures:

Fig. 1 (A): CVs of 1 mmol L^{-1} DA/0.1 mol L^{-1} PBS/pH 7.40 at Pt/PEDOT, Pt/PEDOT/CD-chemically, Pt/PEDOT/CD-electrochemically, Pt/PEDOT/CD-soaking. **(B):** CVs of 1 mmol L^{-1} DA/0.1 mol L^{-1} PBS/pH 7.40 at Pt/PEDOT/NF/CD (dash line) and Au/PEDOT/NF/CD (solid line), scan rate 50 mV s^{-1}.

Fig. 2: CVs of 1 mmol L^{-1} of DA/0.1 mol L^{-1} PBS/pH 7.40 at bare Au, Au/PEDOT/NF, Au/PEDOT, Au/PEDOT/CD and Au/PEDOT/NF/CD, scan rate 50 mV s^{-1}.

Fig. 3: SEM micrographs of **(A)** Au/PEDOT with 50,000 magnification**, (B)** Au/PEDOT/NF/CD with 25,000 magnification, inset; greater magnification 50,000.

Fig. 4: Effect of accumulation time of DA at Au/PEDOT/NF/CD from 0 to 120 s (current I/μA against time t/s)**.**

Fig. 5: DPVs of 15 ml of 0.1 mol L^{-1} PBS/pH 7.40 at Au/PEDOT/NF/CD in different concentrations of DA (2 μmol L^{-1} – 320 μmol L^{-1}). Inset: Calibration curve for DA for concentrations from 2 μmol L^{-1} to 320 μmol L^{-1}.

Fig. 6: (A) DPVs of 300 μmol L^{-1} DA in the presence of 5 mmol L^{-1} AA and 500 μmol L^{-1} UA at bare Au (inset) and Au/PEDOT/NF/CD in the mixture solution (0.1 mol L^{-1} PBS/pH 7.40). **(B)** DPVs of 500 μmol L^{-1} DA in the presence of 1 mmol L^{-1} AA and 500 μmol L^{-1} APAP Au/PEDOT/NF/CD in the mixture solution (0.1 mol L^{-1} PBS/pH 7.40), the inset; DPVs of 1 mmol L^{-1} DA and 1 mmol L^{-1} ST at Au/PEDOT/NF/CD.

Fig. 7: Nyquist plot of Au/PEDOT/NF/CD and bare Au in 1 mmol L^{-1} of DA/0.1 mol L^{-1} PBS/pH 7.40 at the oxidation potential of DA mV. (Symbols and solid lines represent the experimental measurements and the computer fitting of impedance spectra, respectively), frequency range: 0.1–100 000 Hz. Inset, the equivalent circuit used in the fit procedure of the impedance spectra.

List of Tables:

Table 1: Summary of CV results obtained at different modified electrodes for 1 mmol L^{-1} DA in 0.1 mol L^{-1} PBS/pH 7.40, scan rate 50 mV s^{-1}.

Table 2: Comparison for determination of DA at various modified electrodes-based literature reports.

Table 3: Evaluation of the accuracy and precision of the proposed method for the determination of DA in urine sample.

Table 4: EIS fitting data corresponding to Fig. 7 for bare electrode and the proposed sensor.

List of Supplements:

Supplement 1: CVs of 1 mmol L^{-1} of DA/0.1 mol L^{-1} PBS/pH 7.40 at Au/PEDOT/NF/CD at different scan rates (10–200 mV s^{-1}), the inset; linear relationship of I_{pa} vs. $\nu^{1/2}$.

Supplement 2: Linear relationship between the anodic peak potential (mV) vs. the pH values. The inset; the relation between the anodic peak current I_{pa} vs. pH values at Au/PEDOT/NF/CD.

Supplement 3: Stability of Au/PEDOT/NF/CD for 1 mmol L^{-1} of DA/0.1 mol L^{-1} PBS/pH 7.40, 50 repeated cycles.

List of Schemes:

Scheme 1: Schematic representation of the inclusion complex formation between CD and DA, AA and UA as guest molecules.

Table 1

Electrode	E_{pa} mV	I_{pa} µA	ΔE mV	D_{ox} cm^2/s
Bare Au	442	4.33	404	2.07×10^{-6}
Au/PEDOT/NF	350	5.37	300	3.18×10^{-6}
Au/PEDOT	209	16.6	64	3.04×10^{-5}
Au/PEDOT/CD	210	27.5	67	8.34×10^{-5}
Au/PEDOT/NF/CD	220	42.75	75	2.02×10^{-4}

E_{pa}; the anodic peak potential, I_{pa}; the anodic peak current, ΔE; the potential peak separation, D_{app}; the apparent diffusion coefficient.

Table 2

Electrode	LDR (μM)	pH	Sensitivity (μA/μM)	LOD (nM)	Reference
NF/SWCNT/PMT/GCE	5-177	4	0.2649	…	32
β-CD-MWCNTs/Plu-AuNPs/GCE	1.0-56	7	…	190	37
PEDOT…SDS	…	7.4	…	67	13
GCE-CD-PNIPAM	0.1–60	5	0.5642	33.4	36
AuNPs-ß-CD–Gra/GCE	0.5–150	2	NR	150	35
Nafion/$Ni(OH)_2$-MWNTs/GCE	0.05–25	7	1.991	15	33
Au/PEDOT/NF/CD	2–320	7.4	0.1191	2.52	This work

LDR; Linear dynamic range, CD-PNIPAM; β-cyclodextrin-poly(*N*-isopropylacrylamide), GCE; glassy carbon electrode, β-CD-MWCNTs/Plu-AuNPs; Gold nanoparticles-poly(luminol) (Plu-AuNPs) hybrid film and multi-walled carbon nanotubes with incorporated β-cyclodextrin, NF/SWCNT/PMT; a combination of incorporated Nafion, single-walled carbon nanotubes and poly(3-methylthiophene) film, Nafion/$Ni(OH)_2$-MWNTs; Nafion/$Ni(OH)_2$-multiwalled carbon nanotubes.

Table 3

Sample	Concentration of DA added (μmol L^{-1})	Concentration of found DA (μmol L^{-1}) [a]	Recovery (%)	Standard deviation × 10^{-7}	Standard error × 10^{-7}
1	4	3.99	99.75	0.7501	0.4331
2	20	19.77	98.8	1.000	0.5774
3	120	120.3	100.3	0.5000	0.2887
4	280	278.7	99.5	4.726	2.729

[a] Average of five determinations.

Table 4

	Rs Ω cm^2	Cc F cm^{-2}	Rct Ω cm^2	W Ω s$^{-1/2}$	CPE1 F cm^{-2}	n	Cf F cm^{-2}	CPE2 F cm^{-2}	m
Bare Au	254.5	1.085 $\times 10^{-4}$	4210	5.302 $\times 10^{4}$	3.484 $\times 10^{4}$	0.3589	1.426 $\times 10^{-7}$	6.275 $\times 10^{4}$	0.936
Sensor	150.0	1.046 $\times 10^{-9}$	132.3	1.566 $\times 10^{2}$	1.431 $\times 10^{4}$	0.2274	5.541 $\times 10^{-4}$	1.199 $\times 10^{4}$	0.200

Fig. 1 (A)

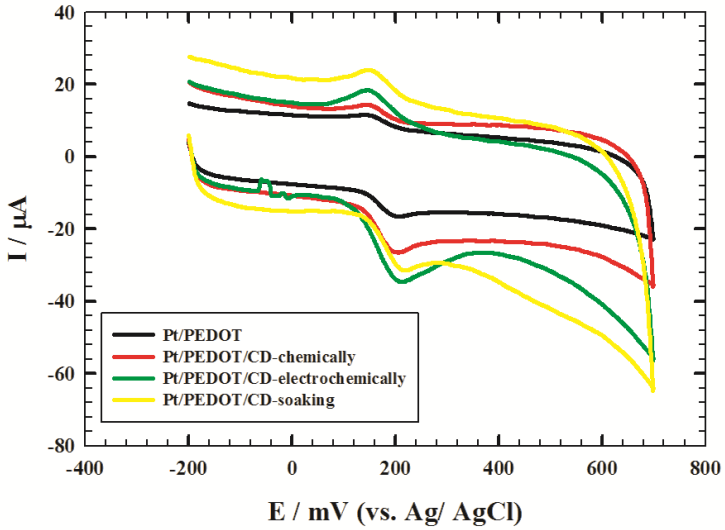

Fig. 1 (B)

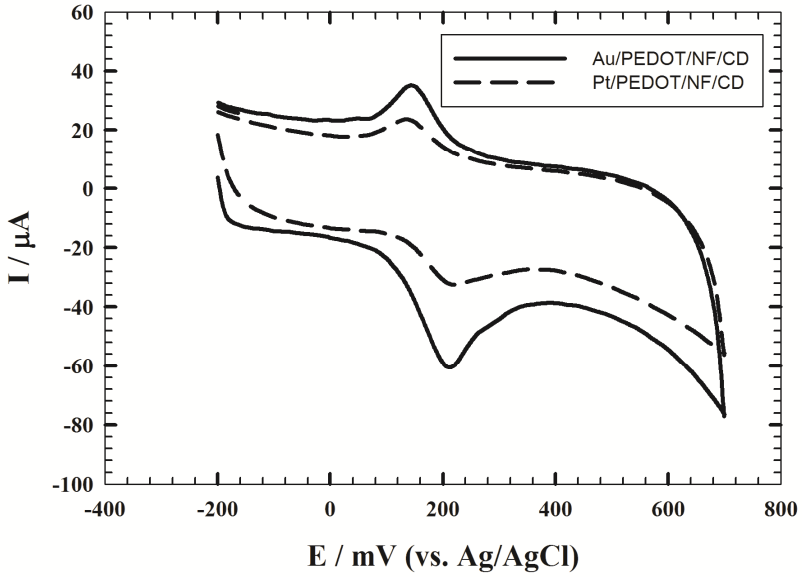

Fig. 2

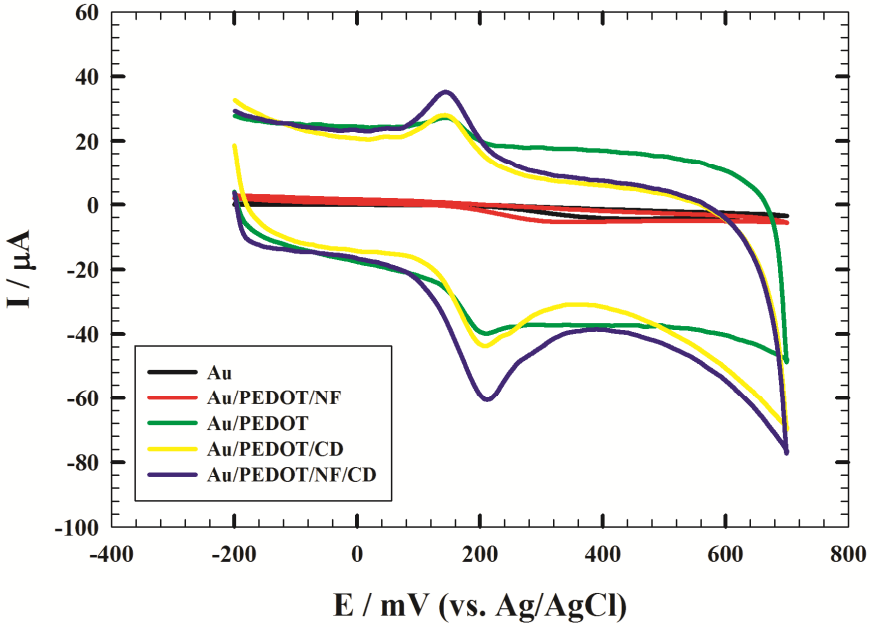

Fig. 3

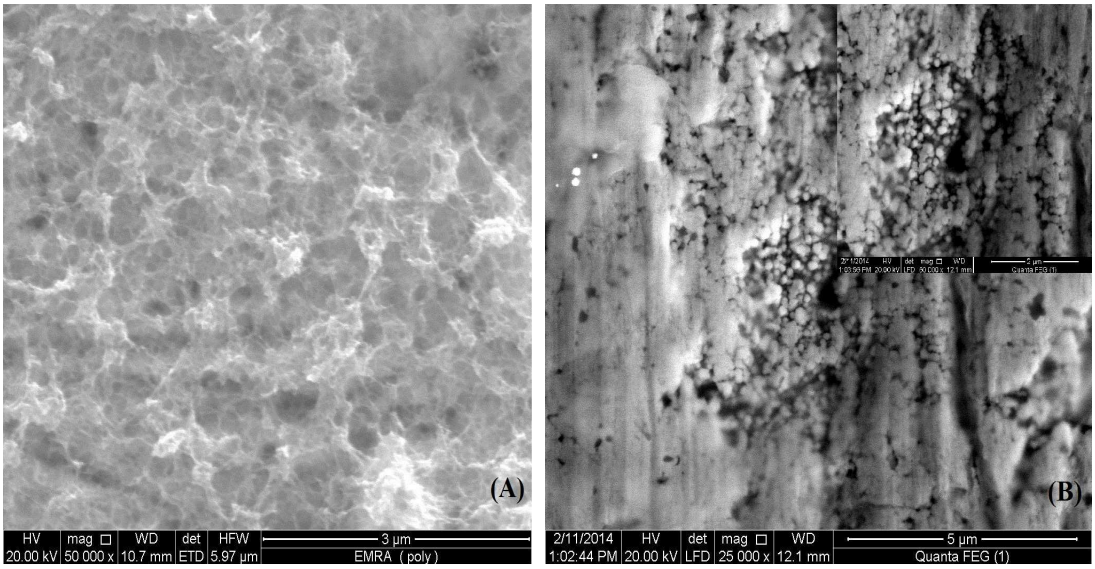

Fig. 4

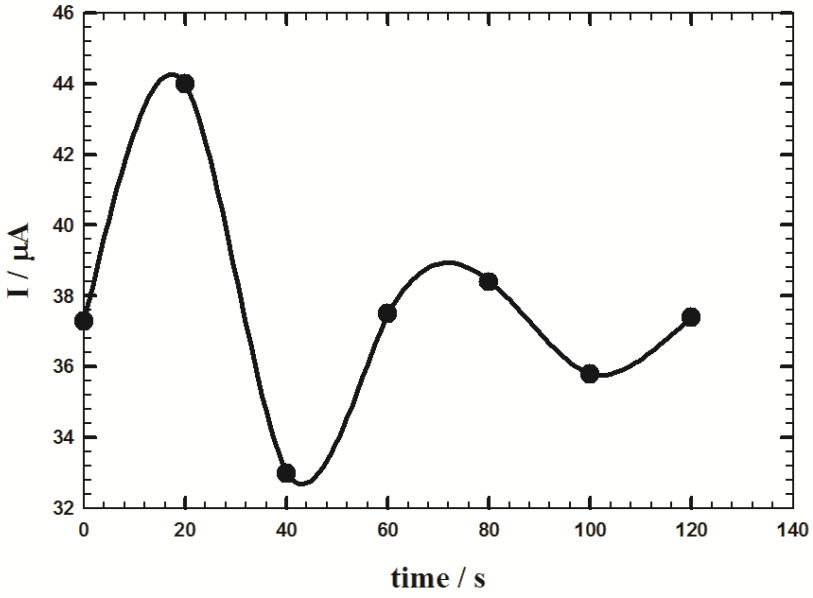

Fig. 5

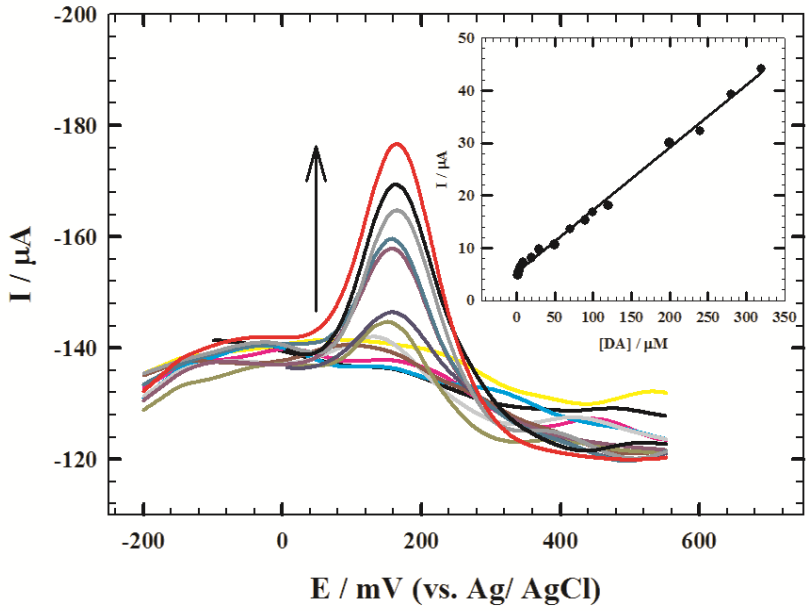

Fig. 6

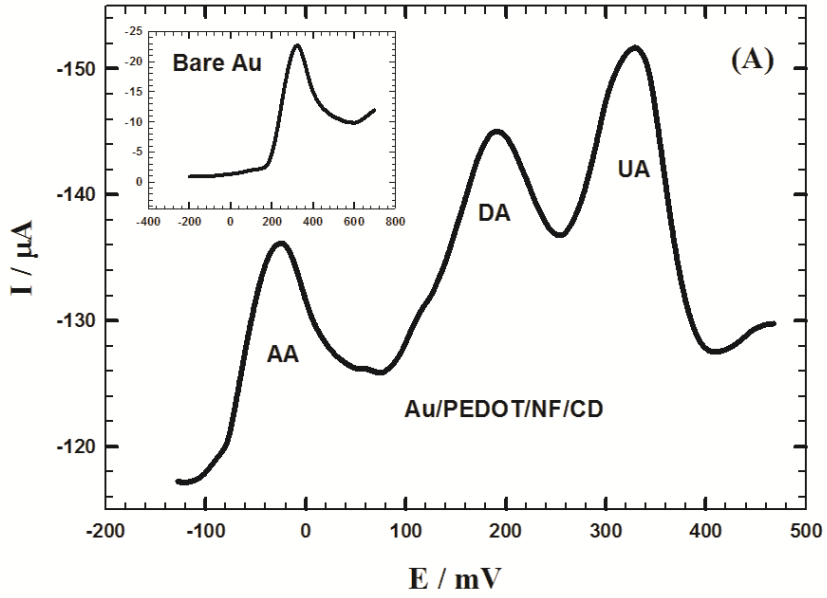

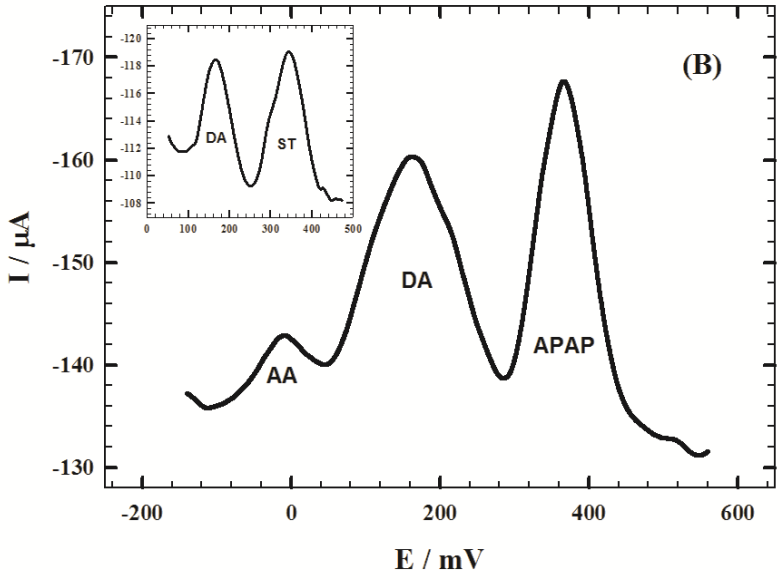

Fig. 7

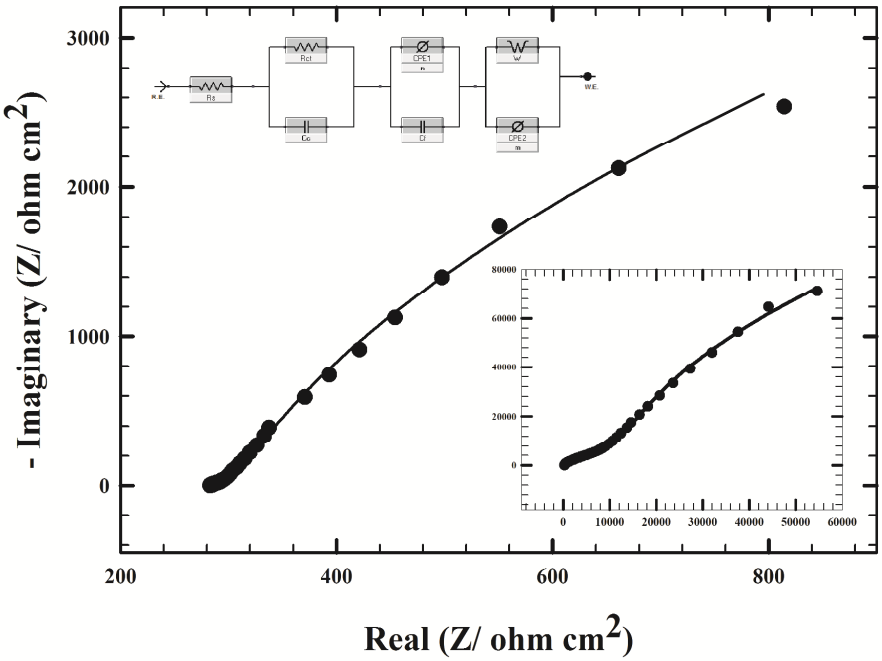

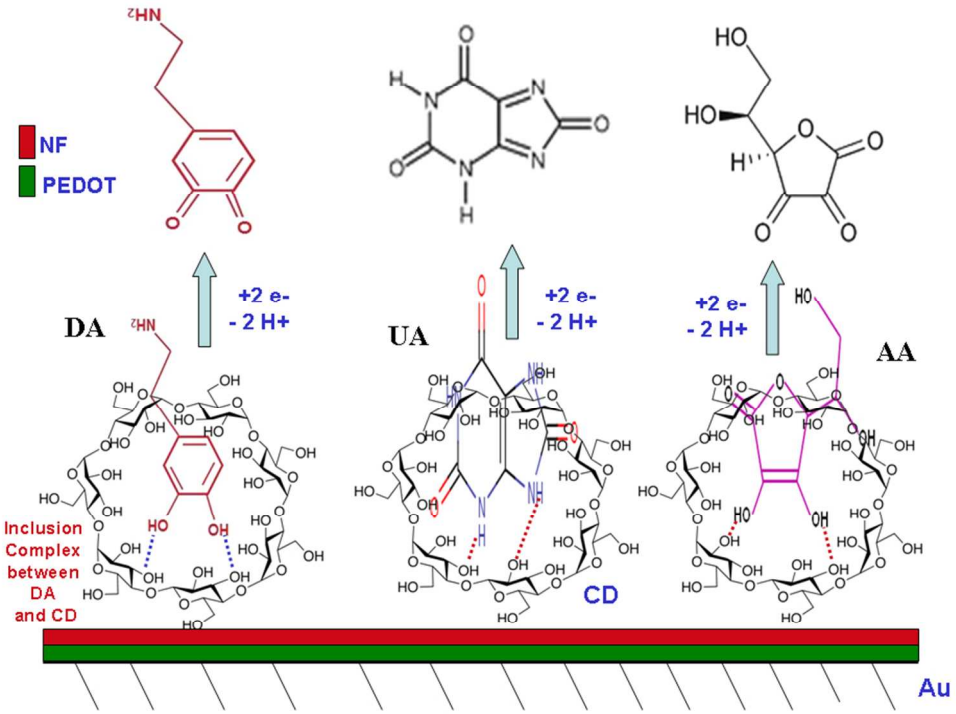

Scheme of drugs inclusion
254x190mm (96 x 96 DPI)